Materials Science and Engineering C 76 (2017) 991–996

Contents lists available at ScienceDirect

Materials Science and Engineering C

journal homepage: www.elsevier.com/locate/msec

# Electrically wired enzyme/$TiO_2$ composite for glucose detection

Joao Henrique Lopes [a], Francois-Xavier Colson [a], Jake E. Barralet [a,b,*,1], Geraldine Merle [c,1]

[a] Faculty of Dentistry, McGill University, Montreal H3A 2B2, Canada
[b] Department of Surgery, Montreal General Hospital, Faculty of Medicine, McGill University, Montreal, Canada
[c] Faculty of Engineering, McGill University, Montreal H3A 2B2, Canada

ARTICLE INFO

*Article history:*
Received 9 October 2016
Received in revised form 17 January 2017
Accepted 15 March 2017
Available online 16 March 2017

*Keywords:*
Electrode
Carbon nanotube
Self-assembly
Electron transfer
Glucose oxidase

ABSTRACT

$TiO_2$, glucose oxidase and carbon nanotube microparticles were ultrasonically formed to provide a large surface area for enzyme immobilisation and a favorable microenvironment for direct electron transfer. This simple architecture nanostructure was used to construct a glucose oxidase biosensor, which demonstrated good analytical performance with high reproducibility, and good detection for pathological glucose level.



## 1. Introduction

Accomplishing a transfer direct of electrons between the active site of an enzyme, and an electrode is a great challenge in the development and commercialization of bioelectrochemical devices such as analyte biosensors or energy production from biofuel cells (BFCs) and other bioelectrocatalytic applications [1]. Direct electron transfer (DET) not only avoids using redox mediators with their associated problems related to the cost, and stability potential but also endeavours to engineer a more simple electrode architectures which could lead to smaller bioelectrochemical systems [2,3]. DET is generally hard to achieve via redox metal centers or tunneling phenomena because of inadequate orientation of the active site of the enzymes to substrates, the burying of active centers inside the protein structure, the denaturation of enzymes resulting from the adsorption, and electrode passivation when the enzyme is immobilised onto the electrodes [2,4]. Mediating DET by engineering bio-electrochemical structures at the nanometer scale is considered one of the most promising approaches. Structured nanomaterials composed of metal oxides [5–7] and conducting polymers [8–10] as well as carbon-based nanomaterials [11,12] such as carbon nanotubes [13–18] and graphene [11,19,20], can possess high electrical conductivity, good biocompatibility, ease of functionalization, and high surface-to-volume ratio. By virtue of the scale of the structure relative to the size of an electrically active site on a protein, they can effectively diminish the electron-tunneling distance to achieve DET of redox enzymes. Considerable work on enzyme immobilisation onto nanostructures has been achieved, nevertheless accomplishing DET without affecting the accessibility of the reactants to the active site whilst providing thermal stability, high catalytic activity and reuse etc., is still challenging. Previously we developed a room temperature self-assembly method [21] that does not require the use of toxic agents allowing enzyme immobilisation during the assembly without altering its native conformation [22]. Among the different bioelectrochemical technologies, enzymatic biosensors and biofuel cells require an efficient electrical contact between electrodes and enzymes and the development of new nanomaterials to perform not only as immobilisation support, but also as electron carrier remains crucial. The majority of the literature on biosensors is related to glucose monitoring with glucose oxidase (GOX) principally for its medical importance in glycemic control [23,24]. Glucose oxidase immobilisation for sensing with DET has previously been achieved through complex architectures [25–28], multistage fabrication processes [29,30], and expensive materials [31–33]. Clinically one of the main issues is reproducibility rather than detection limit since the lower limit of the physiological glucose range is 3.9 mM yet severe hypoglycemia requiring medical intervention is 2.2 mM away at 1.7 mM [34]. Multiple factors related to the biosensor such as design, materials, immobilisation methods can significantly affect the device variability. Thus new, simple, and low cost immobilisation techniques combined with DET that can give consistent electrochemical performance, are of interest. In this work, GOX has been immobilised in one step within microparticles made from $TiO_2$ and carbon nanotubes (CNT) that electrically connect all the components and 'wire' the electrons

* Corresponding author at: Faculty of Dentistry, McGill University, Montreal H3A 2B2, Canada.
*E-mail addresses:* francoisxavier.colson@ensiacet.fr (F.-X. Colson), jake.barralet@mcgill.ca (J.E. Barralet), geraldine.merle@mcgill.ca (G. Merle).
[1] These authors contributed equally.

http://dx.doi.org/10.1016/j.msec.2017.03.113
0928-4931/

from the GOX active site to the metallic support. Efficacy, sensitivity and reproducibility were determined at glucose concentrations up to 3 mM.

## 2. Experimental section

### 2.1. Materials

Titanium Dioxide nanopowder (Aeroxide® P25 $TiO_2$, Ø ~ 20 nm) was supplied by Evonik Industries (Parsippany, NJ), glucose oxidase GOX from Aspergillus Niger (Sigma-Aldrich). All other chemicals used were of reagent grade or better and were supplied by Sigma Aldrich Canada, unless stated otherwise.

### 2.2. Synthesis

#### 2.2.1. Glucose oxidase adsorption

$TiO_2$ and glucose oxidase (GOX) exhibit an isoelectric point of 5.8, and 4.2–4.3 respectively. In order to create opposite charge thereby enhancing the adsorption process between the two materials, a pH of 5 was chosen. GOX from Aspergillus Niger (Sigma Aldrich) was therefore diluted in a potassium phosphate buffer (0.1 M, pH = 5) to obtain a final concentration of 0.2 mg $mL^{-1}$. Both enzyme solution and $TiO_2$ (P25, Degussa, 1 mL per 0.1 g of $TiO_2$) were stirred for 2 h at room temperature, and then kept in the fridge for 12 h before self-assembly process.

#### 2.2.2. Microparticle synthesis

A solution of 1 mg $ml^{-1}$ of carbon nanotubes (carbon nanotube multi walled <50 nm, Sigma Aldrich) in isopropanol was prepared and sonicated for five minutes. Briefly, 2 g of enzymatically modified $TiO_2$ and 12 mL of CNTs solution (1 mg $ml^{-1}$) were mixed together with a final weight ratio of P25/CNT of 0.6 wt%, and 2 mL of $Na_3PO_4$ solution (90 mM) per gram of solid was added. Then the mixture (CNT and GOX/$TiO_2$) was dispersed in isopropanol, and assembled into porous microparticles upon one hour of ultrasound [21]. Finally, the suspension was filtered through a 250 μm and 75 μm sieves and only the particles between 250 and 75 μm diameter were collected and dried. To examine variability from materials synthesis, triplicate measurements of current response with glucose concentration of three CNT/$TiO_2$ microparticle electrodes were performed on three electrodes with three fresh batches of microparticles made with a second batch of enzyme.

### 2.3. Characterisation

All experiments were performed with Milli-Q water (18.2 MΩ·$cm^{-1}$) obtained from an AquaMax-Ultra apparatus. Specific surface area (SSA) determination of $TiO_2$ (P25) nano- and microparticle was performed on a TriStar surface area and porosity analyzer (Micromeritics) using the Brunauer-Emmett-Teller (BET) method of nitrogen adsorption/desorption. Sample morphology was investigated with a SEM FEG Quanta Scanning Electron Microscope (Inspect F50, FEI Company, Hillsboro, OR, USA). Thermogravimetric analyses (TGA) were done with a TA Intruments SDT Q600 TGA/DSC. The samples were heated from 25 °C to 1000 °C in air at 10 °C $min^{-1}$ at flow rate of 100 mL $min^{-1}$. Fourier Transform Infrared Spectroscopy (FTIR) spectrum was obtained using a Perkin Elmer device, Spectrum Two IR spectrometer. Spectrum was measured from 4000 $cm^{-1}$ to 450 $cm^{-1}$. Finally, X-Ray Diffraction (XRD) measurements were realised with a

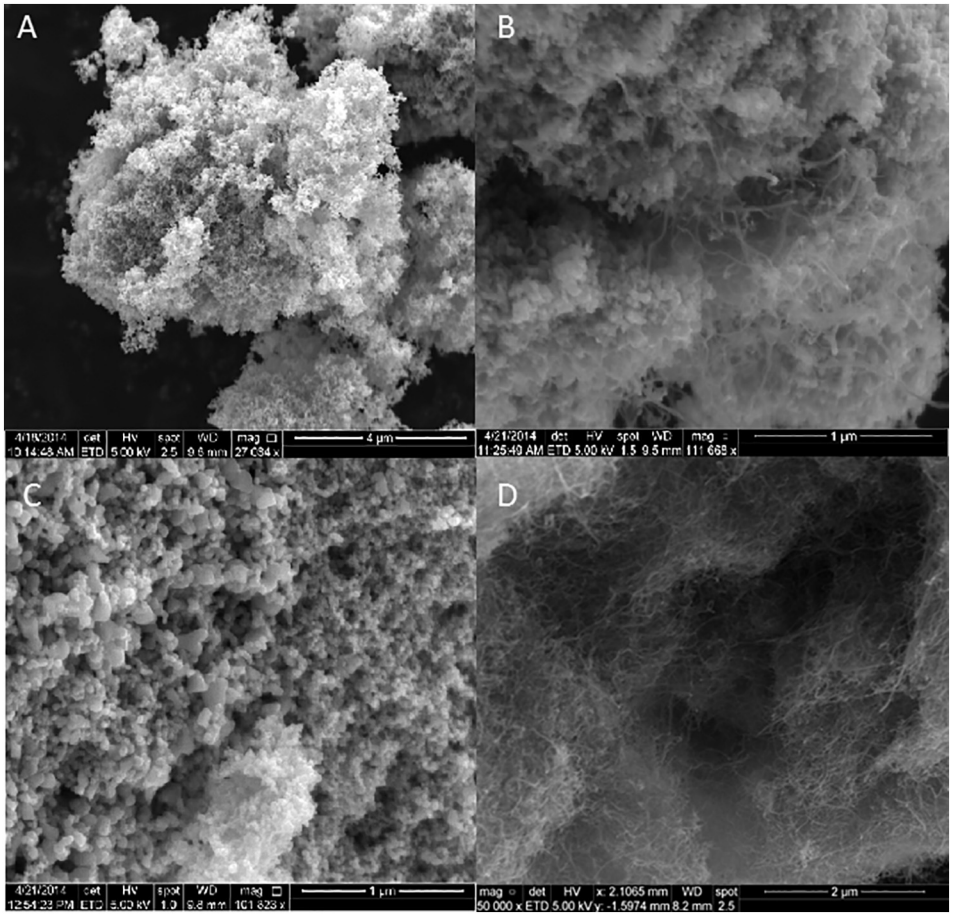


**Fig. 1.** SEM picture at low magnification of the self-assembled CNT/$TiO_2$ microparticles (A), and high magnification of the self-assembled CNT/$TiO_2$ microparticles (B), $TiO_2$ microparticles (C) and commercial carbon nanotubes (D).

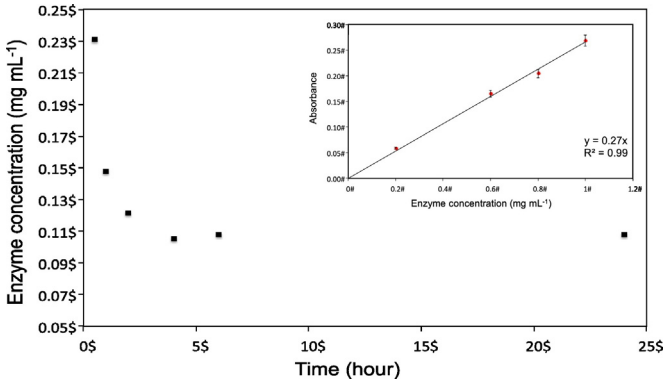


**Fig. 2.** GOX adsorption on the $TiO_2$ function of time by the Bradford method [36] (Inset: GOX calibration curve).

Bruker D8 Discovery X-Ray Diffractometer (VANTEC Detector Cu-Source). Absorbance measurements were realised using a Molecular Devices, Spectramax M2E spectrophotometer. The samples were placed in Suprasil quartz glass cells with a light path of 10 mm. During the adsorption process, a small amount of the supernatant was periodically removed and measured using the Bradford method [35] to measure the concentration of enzyme in solution over the time thereby the enzyme adsorption on the particles. The activity measurements were performed with o-dianisidine (100 μL, (97%, Fisher)) and horseradish peroxidase (100 μL, Fisher, 1kU) in PBS solution (600 μL). The monitoring the absorbance with a UV–Vis spectrophotometer at 440 nm starts after addition of glucose (100 μL). To study the enzymatic stability of the microparticles, samples were kept in a refrigerator at 4 °C in buffer solution at pH 6.8 for 4 weeks. Every 3–4 days supernatant was removed, microparticles were rinsed and the absorbance of the supernatant was measured. Once the measurements were performed, particles were washed three times and then returned to refrigerator. Electrochemical characterisation was performed with a potentiostat VersaSTAT 3, Princeton Applied Research. PBS (0.1 M, pH = 7) (deoxygenated with nitrogen), Pt wire and Saturated Electrode Calomel (SCE) were used as electrolyte, counter and reference electrode respectively. CV scans were performed at a scan rate of 50 mV $s^{-1}$ in the potential range of −0.2–0.60 V (vs. SCE). CV analyses were repeated to determine the stability and the reproducibility of the synthesis. A catalytic ink including P25/CNT/GOX microparticles and Nafion, was drop cast and dried on a glassy carbon electrode. A least squares linear fit of glucose/current relations were plotted in Microsoft Excel to give a line of the form $y = mx + c$ where m is the current density per mM of glucose (A $mM^{-1}$ $cm^{-2}$) and c is a constant current, for each electrode and standard deviations were calculated at each concentration for each electrode. One way ANOVA with Tukey post-hoc test ($P < 0.05$) was performed using the Vassarstats.net online calculator.

## 3. Result and discussion

### 3.1. Characterisation of the CNT/$TiO_2$ microparticles

The morphology of CNT/$TiO_2$ composite microparticles was investigated with SEM (Fig. 1). The three-dimensional microparticles exhibit an open porous structure providing a large surface-to-volume ratio (Fig. 1A), allowing a large amount of enzyme to be immobilised inside as well as on the surface. It can be clearly seen at higher magnification the carbon nanotubes entangled with the $TiO_2$ nanoparticles (Fig. 1C) compared to the pristine $TiO_2$ (Fig. 1B) and commercial carbon nanotubes (Fig. 1D). No shifts in peak positions due to the self-assembly process were observed with XRD measurement (Fig. S1A).

BET analysis shows only a small increase in surface area between the constituent $TiO_2$ nanoparticles (30 $m^2$ $g^{-1}$) and the assembled CNTs/$TiO_2$ microparticles (48 $m^2$ $g^{-1}$). CNT exhibits a SSA of 40–600 $m^2$ $g^{-1}$, thus the increase in SSA for CNTs/$TiO_2$ microparticles is likely the result of the incorporation of the CNTs in the $TiO_2$ microparticles. Knowing the molecular weight of GOX (155 kDa) and its radius (4.3 nm), a maximum of ~$10^{17}$ enzymes per g of CNTs/$TiO_2$ microparticles could be immobilised. Although CNT exhibits a high SSA and could provide the electrical wiring, GOx was not absorbed on CNT because carbon nanotubes alone do not assemble upon ultrasound. The amount of GOX loaded in CNTs/$TiO_2$ microparticles was directly calculated from the measurement of the concentration of GOX in solution using the Bradford method for a 24 h period (Fig. 2) [36].

Fig. 2 represents the amount of GOX in solution The GOX loading on CNTs/$TiO_2$ microparticles due to the high specific surface area and the electrostatic interaction between the $TiO_2$ and GOX at pH 5 was relative fast after 4 h (Fig. 1D). After 5 h, 92.1 mg of GOX was immobilised in 1 g of microparticles. The presence of the enzyme in the CNTs/$TiO_2$ microparticles after ultrasonic welding was confirmed with FTIR spectroscopy. (Supplementary information Fig. S1). 1651 $cm^{-1}$, 1393 $cm^{-1}$ and 1095 $cm^{-1}$ peaks correspond to the amide I, the C—H bending and the C—O stretching of the enzyme respectively [37].

### 3.2. Catalytic activity of the CNTs/$TiO_2$/GOX microparticles

The biocatalytic activities of GOX in solution (free) and GOX immobilised on microparticles were investigated by monitoring the oxidation of glucose in the presence of horseradish peroxidase. The enzymatic activities of the free and immobilised GOX were determined for a given enzyme concentration. The kinetic parameters such as maximum rate at which the enzyme can perform (Rm) and the Michaelis constant (Km) for the free GOX and immobilised enzyme were calculated from the Lineweaver — Burk plots (Fig. 3) following the Eq. (1):

$$\frac{1}{V} = \frac{Km}{V\,max} \times \frac{1}{[S]} + \frac{1}{V\,max} \tag{1}$$

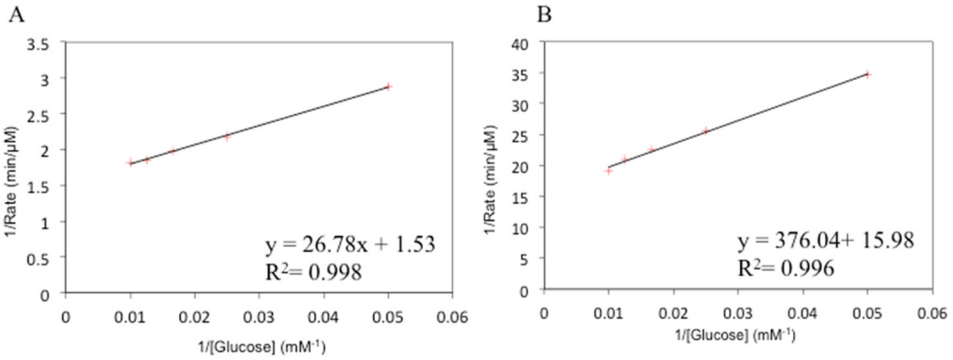


**Fig. 3.** Lineweaver–Burk plots of free (A) and immobilised GOX (B).

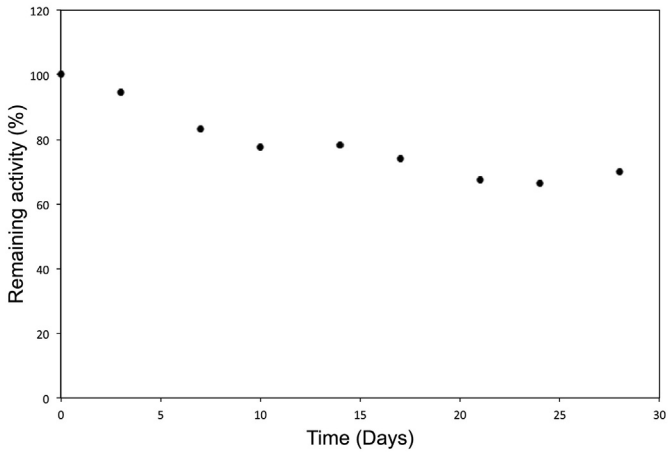


**Fig. 4.** Remaining activity of immobilised GOX modified microparticles over time at 4 °C.

where V is the reaction velocity, Km is the Michaelis–Menten constant, Vmax is the maximum reaction velocity, and [S] is the substrate concentration.

A Km value of approximately 17.5 mM and 23.5 mM was found for free and immobilised GOX respectively, confirming that the ultrasonic process and the nano-environment do not alter the affinity of the enzyme for the substrate. However, a Vmax for the immobilised GOX (0.063 μM/min) was found to be ten times lower than the free enzyme (0.65 μM/min).

Although adsorption of GOX and CNTs/$TiO_2$ microparticles has shown no conformational change of the enzyme or destruction of its active center, with a Km values between free and immobilised enzyme comparable (23.5 vs. 17.5 mM). When GOX is immobilised in the CNTs/$TiO_2$ microparticles, there are interactions, which are mainly by hydrogen bonds, multiple salt linkages, and Van der Waal's forces between GOX and CNTs/$TiO_2$ microparticles that can hamper the accessibility of the active site for the substrate as well as slow down the diffusion of the substrate and the product to the enzyme and the solution respectively. Fig. 4 shows the storage stability for the immobilised enzyme within CNTs/$TiO_2$ microparticles at 4 °C in PBS buffer (50 mM, pH 5), physiological conditions where no activity loss was recorded for the free enzyme. The residual activity for the modified CNTs/TiO2 microparticle remained high after 30 days with a gradual decrease up to 30% of its initial activity after 30 days storage (Fig. 4). This mild decrease of catalytic activity may have been as a consequence of the desorption of a small amount of enzyme from the microparticles resulting in a leaching of the enzyme.

### 3.3. Direct electrochemistry of glucose oxidase

In order to examine the electron transfer, the electrochemical behaviour of $TiO_2$/CNTs/GOX microparticles was investigated using cyclic voltammetry (Fig. 4).

Cyclic voltammograms were recorded in the potential range of −0.2 to −0.6 V. In the absence of GOX (Fig. 5A), no significant redox peaks were noticed in this potential range for $TiO_2$/CNTs microparticle electrode. However, the $TiO_2$/CNTs/GOX electrode exhibits a pair of well-defined redox peaks at ~ −0.46 V, related to GOX and more specifically to the redox active center (FAD/$FADH_2$) (Fig. 5A). The peak-to-peak separation of cathodic to anodic current intensity was roughly 80 mV, indicating a rapid electron transfer, probably due to the large surface area of the $TiO_2$ nanoparticle and the CNTs and fast electron communication resulting from the assembly of CNTs with $TiO_2$ (Supplementary information Fig. S2A). The oxidation peak current versus the scan rate displayed a linear relationship, indicating that the electron transfer reaction of the FAD/$FADH_2$ active center is a surface-controlled electrochemical process [38] (Fig. S2B). The CV of the bioelectrode in $N_2$-saturated and air-saturated PBS shows that the reduction current decreases in the presence of oxygen, suggesting that the $TiO_2$/CNTs/GOX microparticles catalyze the reduction of $O_2$ (Fig. 5B). This result shows that the Oxygen Reduction Reaction is catalyzed at the $TiO_2$/CNTs/GOX electrode by GOX [39], through a direct electron transfer process as follows:

$$2\text{GOX-FADH}_2 + \text{O}_2 \rightarrow 2\text{GOX-FAD} + 2\text{H}_2\text{O}$$

However, when glucose is added in the air saturated PBS, the cathodic peak current decreases because of the enzymatic reaction between the oxidized form of GOX and glucose thereby restrained the electroreduction of $O_2$. This confirms the key role of the CNTs assembled with $TiO_2$ in promoting successfully the direct electron transfer between GOX and the electrode surface.

### 3.4. Detecting glucose at the $TiO_2$/CNTs/GOX microparticle electrode

Then, detection of glucose by the prepared biosensor was investigated by amperometric method and the reproducibility of the processing method assessed independently with cyclic voltammetry. The experiment was realised in air-saturated PBS 0.1 M (pH = 7) and from Fig. 5 an applied potential was chosen at E = −0.4 V to facilitate the GOX re-oxidation [24]. After waiting for the stabilisation of the signal, glucose was added to the stirred PBS successively (in order to obtain a range between 100 μM and 400 μM of glucose) and the maximal increase of the reduction current was observed each time (Fig. S3). Indeed, as glucose

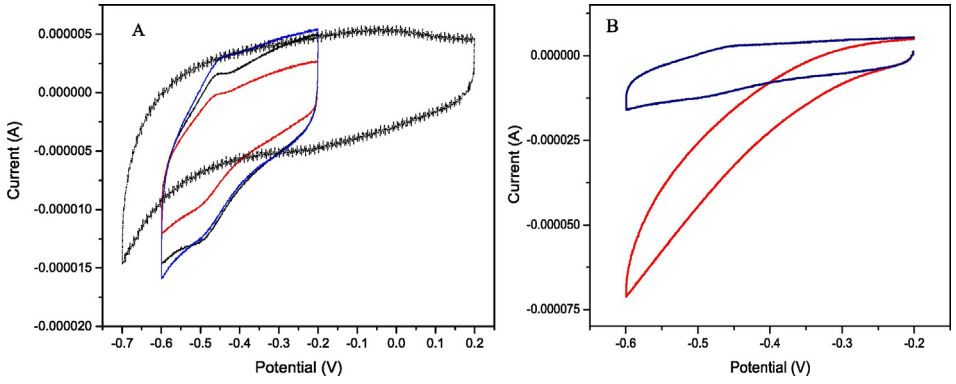


**Fig. 5.** (A) Cyclic voltammograms of 3 electrodes modified with GOX/$TiO_2$/CNTs synthesized at different time with electrode modified with $TiO_2$/CNTs (black curve) and (B) Cyclic voltammograms comparison of GOX/$TiO_2$/CNTs electrode in $N_2$-saturated (blue) and air-saturated (red) pH 7.4 PBS. (For interpretation of the references to colour in this figure legend, the reader is referred to the web version of this article.)

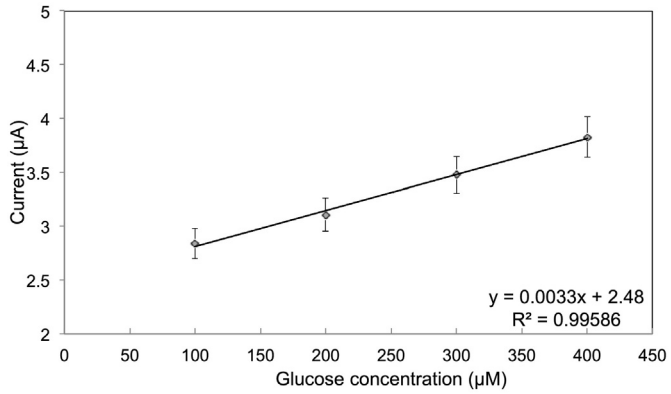


**Fig. 6.** Linear relationship of steady-state currents versus glucose concentrations.

was added to PBS, the reduction current increased because of consumption of glucose in oxidation reaction to gluconolactone following [40]:

$$GOX\ (FAD) + Glucose \rightarrow GOX\ (FADH_2) + Gluconolactone$$

From the amperometric measurement, a calibration curve was done (Fig. 6) and showed that the current increase was proportional to the glucose concentration in solution from 100 to 400 μM. Thus, from this curve, the glucose concentration from an unknown sample can now be determined.

From Fig. 6, based on the calculated slope (3.3 $\mu A.mM^{-1}$) and the area of the electrode (0.19 $cm^2$), the glucose biosensor exhibited a sensitivity of 17.16 $\mu A\ mM^{-1}\ cm^{-2}$ comparable with other expensive and more complex systems using osmium and gold materials (in Supplementary information Table S1). Moreover the selectivity of the $TiO_2$/CNTs microparticle biosensor was studied with the addition of 0.5 mM of acid ascorbic and 0.5 mM of acid aspartic in a 0.1 M PBS during the amperometric measurement. No detectable change in the signal was observed whereas an oxidation current is directly measured after a simple addition of 0.5 mM of glucose (in Supplementary information, Fig. S3B). The reproducibility of the GOX/$TiO_2$/CNTs bioelectrode towards glucose was investigated. The bioelectrodes were remade ($N = 3$) and the current response for each electrode was measured on three separate occasions, an average sensitivity of $11.3 \pm 1.3\ \mu A\ mM^{-1}\ cm^{-2}$ was calculated (Fig. S4). There was no significant difference (ANOVA, Tukey posthoc, $P < 0.05$) between the values at a given glucose concentration for any electrode, confirming reproducibility. Whether normalized to the current value at 0 mM glucose or not, (Fig. 7), current

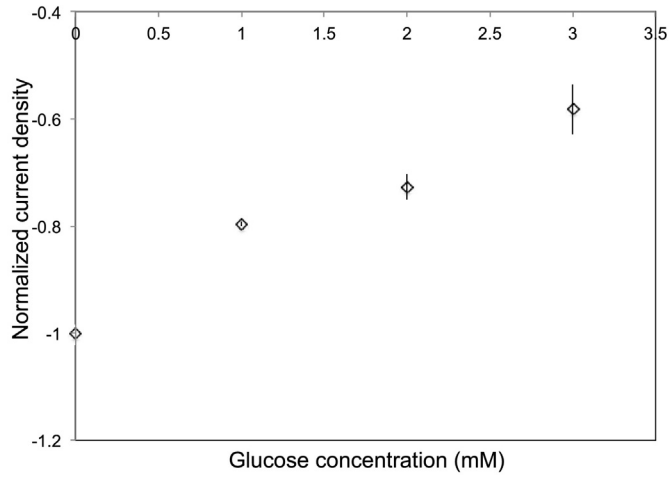


**Fig. 7.** Normalized current density at 400 mV versus glucose concentrations of GOX/$TiO_2$/CNTs electrodes.

values were significantly different, (ANOVA, Tukey Posthoc, $P < 0.05$), between all glucose concentrations, except between 1 and 2 mM, ($P = 0.051$).

According to Eqs. (2) and (3) [41]:

$$y_{LOD} = yblank + t_{\alpha,k-1} s_y \quad (2)$$

$$x_{LOD} = \frac{ts_y}{m} \quad (3)$$

Where y is current and x is concentration, LOD is limit of detection, $t_{\alpha,\ k-1}$ is the Student's *t*-function with $k - 1$ degrees of freedom and $\alpha = 0.05$, $s_y$ standard deviation and m is the slope, the LODs were $-74.6\ \mu A/cm^2$ and 0.96 mM, similar to values for enzymatic colourimetric techniques [42]. Although GOX immobilised on carbon nanotubes [43] or graphene [44] with functionalized ionic liquid (PFIL) have shown a direct electron transfer, they generally obtained a response in the milli molar range limiting their application to the determination of blood sugar concentration in normal condition (4-6 mM). Slightly reducing the response range to 0.1 mM has been achieved either with a more sophisticated approach including Au nanoparticles [45], CdS [46], a multilayer films via layer-by-layer self-assembly of multiwall carbon nanotubes [30], or by simple casting process with Nafion, GOX and carbon nanotubes (0.25 mM) [47]. The latter lead to the detection at a positive potential of 0.7 V, which could interfere with some other related biomolecules. A detection range of 0.010–1.42 mM associated with a low limit of detection of 10 μm and a sensitivity of 5.32 $\mu A\ mM^{-1}\ cm^{-2}$ has been described with $TiO_2$-SWNCT electrode [16]. This sensor exhibits a nanowire-structured composite with a high porosity fabricated by the deposition of SWCNTs on ITO using a simple arc discharge followed by $TiO_2$ coating via MOCVD. Here, our $TiO_2$/CNTs biosensor exhibits comparable sensitivity for the glucose detection at a high selectivity with a simpler and cheaper processing method with a good reproducibility.

## 4. Conclusion

In summary, CNTs/$TiO_2$ composite microparticles, prepared in one step synthesis, exhibited good electronic properties and biocompatibility. GOX was immobilised into this composite during the self-assembly process. This novel architecture achieved successfully the direct electron transfer between the FADH/FAD redox center of the enzyme and the electrode surface and maintained strongly the bioactivity of the enzyme. Finally, we have successfully tested this material for the electrochemical detection of glucose, and prove that it could become a potential possibility for the further fabrication of biosensors. In conclusion, we proved that our ultrasonic mediated fabrication process can generate robust microparticles from a variety of materials, which can be easily tuned for use with different enzymes and electrochemical applications.

## Acknowledgements

This work was carried out with the support of the São Paulo Research Foundation – FAPESP (Grant 2013/12376-5). Natural Sciences and Engineering Research Council of Canada (NSERC) is acknowledged for the funding of a Discovery Grant (JB) and a Strategic Grant (JB). The manuscript was written through contributions of all authors. All authors have given approval to the final version of the manuscript.

## Appendix A. Supplementary data

Supporting information is available from the Wiley Online Library or from the author. Supplementary data associated with this article can be found in the online version, at http://dx.doi.org/10.1016/j.msec.2017.03.113.

## References


[1] M. Falk, Z. Blum, S. Shleev, Direct electron transfer based enzymatic fuel cells, Electrochim. Acta 82 (2012) 191–202.
[2] M. Zhao, Y. Gao, J. Sun, F. Gao, Mediatorless glucose biosensor and direct electron transfer type glucose/air biofuel cell enabled with carbon nanodots, Anal. Chem. 87 (5) (2015) 2615–2622.
[3] B. Liang, L. Fang, G. Yang, Y. Hu, X. Guo, X. Ye, Direct electron transfer glucose biosensor based on glucose oxidase self-assembled on electrochemically reduced carboxyl graphene, Biosens. Bioelectron. 43 (2013) 131–136.
[4] J. Wang, Electrochemical sensors, Analytical Electrochemistry, John Wiley & Sons, Inc. 2006, pp. 201–243.
[5] P.R. Solanki, A. Kaushik, V.V. Agrawal, B.D. Malhotra, Nanostructured metal oxide-based biosensors, NPG Asia Mater. 3 (2011) 17–24.
[6] A.K. Gupta, M. Gupta, Synthesis and surface engineering of iron oxide nanoparticles for biomedical applications, Biomaterials 26 (18) (2005) 3995–4021.
[7] R.-a. Doong, H.-m. Shih, Array-based titanium dioxide biosensors for ratiometric determination of glucose, glutamate and urea, Biosens. Bioelectron. 25 (6) (2010) 1439–1446.
[8] A. Macagnano, E. Zampetti, E. Kny, Electrospinning for High Performance Sensors, Springer International Publishing, 2015.
[9] T.A. Skotheim, J. Reynolds, Handbook of Conducting Polymers, CRC Press, 2007 (2 Volume Set).
[10] N.C. Foulds, C.R. Lowe, Enzyme entrapment in electrically conducting polymers. Immobilisation of glucose oxidase in polypyrrole and its application in amperometric glucose sensors, J. Chem. Soc., Faraday Trans. 1 82 (4) (1986) 1259–1264.
[11] W. Putzbach, N.J. Ronkainen, Immobilization techniques in the fabrication of nanomaterial-based electrochemical biosensors: a review, Sensors (Basel, Switzerland) 13 (4) (2013) 4811–4840.
[12] M. Wooten, S. Karra, M. Zhang, W. Gorski, On the direct electron transfer, sensing, and enzyme activity in the glucose oxidase/carbon nanotubes system, Anal. Chem. 86 (1) (2014) 752–757.
[13] F. Patolsky, Y. Weizmann, I. Willner, Long-range electrical contacting of redox enzymes by SWCNT connectors, Angew. Chem. Int. Ed. 43 (16) (2004) 2113–2117.
[14] J. Ryu, H. Kim, S. Lee, H.T. Hahn, D. Lashmore, Carbon nanotube mat as mediator-less glucose sensor electrode, J. Nanosci. Nanotechnol. 10 (2) (2010) 941–947.
[15] S.P. Kim, H.C. Choi, Reusable hydrazine amperometric sensor based on Nafion®-coated TiO2–carbon nanotube modified electrode, Sensors Actuators B Chem. 207 Part A (2015) 424–429.
[16] N.Q. Dung, D. Patil, T.T. Duong, H. Jung, D. Kim, S.-G. Yoon, An amperometric glucose biosensor based on a GOx-entrapped TiO2–SWCNT composite, Sensors Actuators B Chem. 166–167 (2012) 103–109.
[17] M. Tasviri, H.-A. Rafiee-Pour, H. Ghourchian, M.R. Gholami, Amine functionalized TiO2 coated on carbon nanotube as a nanomaterial for direct electrochemistry of glucose oxidase and glucose biosensing, J. Mol. Catal. B Enzym. 68 (2) (2011) 206–210.
[18] Y.-H. Wang, F.-L. Li, Y.-Q. Wang, S. Wu, X.-X. He, K.-M. Wang, A TiO2/CNTs nanocomposites enhanced luminol electrochemiluminescence assay for glucose detection, Chin. J. Anal. Chem. 43 (11) (2015) 1682–1687.
[19] L. Wang, M. Xu, L. Han, M. Zhou, C. Zhu, S. Dong, Graphene enhanced electron transfer at aptamer modified electrode and its application in biosensing, Anal. Chem. 84 (17) (2012) 7301–7307.
[20] Y. Song, C. Chen, C. Wang, Graphene/enzyme-encrusted three-dimensional carbon micropillar arrays for mediatorless micro-biofuel cells, Nano 7 (16) (2015) 7084–7090.
[21] D.C. Bassett, G. Merle, B. Lennox, R. Rabiei, F. Barthelat, L.M. Grover, J.E. Barralet, Ultrasonic phosphate bonding of nanoparticles, Adv. Mater. 25 (41) (2013) 5953–5958.
[22] G. Merle, M. Seon-Lutz, J.H. Lopes, J.E. Barralet, Hierarchical stable enzyme microenvironments for high-temperature stability in amine solvents, Part. Part. Syst. Charact. 31 (10) (2014) 1091–1096.
[23] L.F. Ang, L.Y. Por, M.F. Yam, Development of an amperometric-based glucose biosensor to measure the glucose content of fruit, PLoS One 10 (3) (2015), e0111859.
[24] S. Ferri, K. Kojima, K. Sode, Review of glucose oxidases and glucose dehydrogenases: a bird's eye view of glucose sensing enzymes, J. Diabetes Sci. Technol. 5 (5) (2011) 1068–1076.
[25] J. Huang, L. Zhang, R.-P. Liang, J.-D. Qiu, "On-off" switchable electrochemical affinity nanobiosensor based on graphene oxide for ultrasensitive glucose sensing, Biosens. Bioelectron. 41 (2013) 430–435.
[26] Y.-Q. Zhang, Y.-J. Fan, L. Cheng, L.-L. Fan, Z.-Y. Wang, J.-P. Zhong, L.-N. Wu, X.-C. Shen, Z.-J. Shi, A novel glucose biosensor based on the immobilization of glucose oxidase on layer-by-layer assembly film of copper phthalocyanine functionalized graphene, Electrochim. Acta 104 (2013) 178–184.
[27] L. Zhou, Y. Jiang, J. Gao, X. Zhao, L. Ma, Q. Zhou, Oriented immobilization of glucose oxidase on graphene oxide, Biochem. Eng. J. 69 (2012) 28–31.
[28] M. Zhang, C. Liao, C.H. Mak, P. You, C.L. Mak, F. Yan, Highly sensitive glucose sensors based on enzyme-modified whole-graphene solution-gated transistors, Sci. Rep. 5 (2015) 8311.
[29] H. Yin, Y. Zhou, X. Meng, K. Shang, S. Ai, One-step "green" preparation of graphene nanosheets and carbon nanospheres mixture by electrolyzing graphite rob and its application for glucose biosensing, Biosens. Bioelectron. 30 (1) (2011) 112–117.
[30] W. Zhang, Y. Du, M.L. Wang, On-chip highly sensitive saliva glucose sensing using multilayer films composed of single-walled carbon nanotubes, gold nanoparticles, and glucose oxidase, Sens. Biosensing Res. 4 (2015) 96–102.
[31] J. Du, X. Yu, J. Di, Biosens. Bioelectron. 7 (2012).
[32] C. Qiua, X. Wang, X. Liub, S. Houc, H. Ma, Electrochim. Acta 67 (2012).
[33] Y.-F. Bai, T.-B. Xu, J.H.T. Luong, H.-F. Cui, Direct electron transfer of glucose oxidase-boron doped diamond Interface: a new solution for a classical problem, Anal. Chem. 86 (10) (2014) 4910–4918.
[34] K. Tonyushkina, J.H. Nichols, Glucose meters: a review of technical challenges to obtaining accurate results, J. Diabetes Sci. Technol. 3 (4) (2009) 971–980 (Online).
[35] M. Vinoba, K.S. Lim, S.H. Lee, S.K. Jeong, M. Alagar, Immobilization of human carbonic anhydrase on gold nanoparticles assembled onto amine/thiol-functionalized mesoporous SBA-15 for biomimetic sequestration of CO2, Langmuir 27 (10) (2011) 6227–6234.
[36] M.M. Bradford, A rapid and sensitive method for the quantitation of microgram quantities of protein utilizing the principle of protein-dye binding, Anal. Biochem. 72 (1) (1976) 248–254.
[37] J. Hui, J. Cui, G. Xu, S.B. Adeloju, Y. Wu, Direct electrochemistry of glucose oxidase based on Nafion-graphene-GOD modified gold electrode and application to glucose detection, Mater. Lett. 108 (2013) 88–91.
[38] W. Tang, L. Li, L. Wu, J. Gong, X. Zeng, Glucose biosensor based on a glassy carbon electrode modified with polythionine and multiwalled carbon nanotubes, PLoS One 9 (5) (2014), e95030.
[39] C.X. Guo, C.M. Li, Direct electron transfer of glucose oxidase and biosensing of glucose on hollow sphere-nanostructured conducting polymer/metal oxide composite, Phys. Chem. Chem. Phys. 12 (38) (2010) 12153–12159.
[40] A.A. Sehat, A.A. Khodadadi, F. Shemirani, Y. Mortazavi, Fast immobilization of glucose oxidase on graphene oxide for highly sensitive glucose biosensor fabrication, Int. J. Electrochem. Sci. 10 (1) (2015) 272–286.
[41] H.-P. Loock, P.D. Wentzell, Detection limits of chemical sensors: applications and misapplications, Sensors Actuators B Chem. 173 (2012) 157–163.
[42] A.L. Galant, R.C. Kaufman, J.D. Wilson, Glucose: detection and analysis, Food Chem. 188 (2015) 149–160.
[43] A. Salimi, B. Kavosi, R. Hallaj, A. Babaei, Fabrication of a highly sensitive glucose biosensor based on immobilization of osmium complex and glucose oxidase onto carbon nanotubes modified electrode, Electroanalysis 21 (8) (2009) 909–917.
[44] C. Shan, H. Yang, J. Song, D. Han, A. Ivaska, L. Niu, Direct electrochemistry of glucose oxidase and biosensing for glucose based on graphene, Anal. Chem. 81 (6) (2009) 2378–2382.
[45] B.P. Crulhas, J.R. Sempionatto, M.F. Cabral, S. Minko, V.A. Pedrosa, Stimuli-responsive Biointerface based on polymer brushes for glucose detection, Electroanalysis 26 (4) (2014) 815–822.
[46] J. Qian, S. Yan, Z. Xiao, Electrochemical biosensor based on CdS nanostructure surfaces, J. Colloid Interface Sci. 366 (1) (2012) 130–134.
[47] X.-H. Pham, M.-P.N. Bui, C.A. Li, K.N. Han, J.H. Kim, H. Won, G.H. Seong, Electrochemical characterization of a single-walled carbon nanotube electrode for detection of glucose, Anal. Chim. Acta 671 (1–2) (2010) 36–40.